

Dynamic all-optical tuning of transverse resonant cavity modes in photonic bandgap fibers

Gilles Benoit, Ken Kuriki, Jean-Francois Viens, John D. Joannopoulos, and Yoel Fink

Center for Materials Science and Engineering, Research Laboratory of Electronics,
Massachusetts Institute of Technology, Cambridge, Massachusetts, 02139

Received January 3, 2005

Photonic bandgap fibers for transverse illumination containing half-wavelength microcavities have recently been designed and fabricated. We report on the fabrication and characterization of an all-optical tunable microcavity fiber. The fiber is made by incorporating a photorefractive material inside a Fabry–Perot cavity structure with a quality factor $Q > 200$ operating at $1.5 \mu\text{m}$. Under short-wavelength transverse external illumination, a 2 nm reversible shift of the cavity resonant mode is achieved. Dynamic all-optical tuning is reported at frequencies up to 400 Hz. Experimental results are compared with simulations based on the amplitude and kinetics of the transient photodarkening effect measured *in situ* in thin films. © 2005 Optical Society of America

OCIS codes: 060.4080, 160.5320.

Fibers with multiple radial alternating submicrometer layers of high-index amorphous semiconductor and low-index polymer containing half-wavelength defect layer microcavities¹ have recently been shown to exhibit optical resonant modes for transverse illumination.² Their nearly cylindrical geometry lends itself to mechanical and optical tuning of the respective resonant modes^{2,3} and presents significant opportunities for fabrication of devices such as tunable dispersion compensators⁴ on a kilometer length scale. We recently demonstrated mechanical tuning of a microcavity fiber with a reversible shift under 0.9% applied axial strain of 0.35% of the spectral position of cavity resonant modes with a quality factor $Q \sim 35$.² Here we report on the fabrication of fibers containing optical cavities with $Q > 200$ made from a highly photorefractive glass arsenic triselenide (As_2Se_3) and surrounded by alternating polyetherimide (PEI) and arsenic trisulfide (As_2S_3) mirror layers. We demonstrate reversible all-optical tuning of the cavity resonant mode of these fibers based on the transient refractive-index change exhibited by As_2S_3 and As_2Se_3 amorphous thin films illuminated at 514 nm.

As_2S_3 and As_2Se_3 are two chalcogenide glasses known for exhibiting photodarkening, an illumination-induced redshift of the optical absorption edge commensurate with an increase of the real part of the refractive index (n) through the Kramers–Kronig relations.⁵ Photodarkening consists of a metastable and a transient part that can be well described by the so-called slip and repulsion model.⁶ Metastable photodarkening (MP), reversible only by annealing near the glass transition temperature, involves photoassisted site switching that is responsible for an increase in structural disorder, while transient photodarkening (TP), which is fully reversible at room temperature, involves nonradiative recombination of photoexcited charge carriers and defects.⁶ To characterize this transient index change in As_2Se_3 and As_2S_3 thin films under illumina-

tion with a (Coherent Innova 90 plus) Ar^+ laser emitting at 514 nm, we first measured the amplitude of TP by use of a Sopra GES-5 spectroscopic ellipsometer⁷ and then measured its kinetics by performing *in situ* transmission measurements at $1.5 \mu\text{m}$ using a Photonics Tunics plus laser (10 mW). While transmission and ellipsometry measurements have been used separately to characterize MP^{8,9} and the transient change in k ,⁶ no similar *in situ* characterization has been reported to our knowledge. We deposited 100-nm-thick As_2Se_3 and As_2S_3 films under vacuum (2×10^{-5} Torr) with a Ladd Industries thermal evaporator and annealed them for 2 h under vacuum at 180°C before measurement. The amplitude of TP in As_2Se_3 and As_2S_3 films deposited on a Si substrate was measured at saturation 2 h after the illumination was turned on under illumination power of up to 1 W/cm^2 . The saturated MP at $1.5 \mu\text{m}$ was found to be equal to 2.7% and 1.3% of the annealed refractive index for As_2Se_3 and As_2S_3 , respectively. TP at $1.5 \mu\text{m}$ increased linearly with increasing intensity before saturating at $\sim 3.7\%$ and $\sim 1\%$ for As_2Se_3 and As_2S_3 , respectively. The intensity dependence of the kinetics of the TP in As_2Se_3 and As_2S_3 thin films deposited on VWR glass slides was determined by fitting transmission spectra recorded over time [Fig. 1(a)] with a stretched exponential function⁶:

$$T(t) = T_0 - \Delta T_{\text{max}} \exp[-(t/\tau)^\beta],$$

where T_0 is the initial transmission, ΔT_{max} is the maximum change in transmission, τ is the characteristic time, and β is the characteristic dispersion parameter ($0 < \beta < 1$). On average we obtained $\beta_{\text{As}_2\text{Se}_3} = 0.79$ and $\beta_{\text{As}_2\text{S}_3} = 0.96$. The characteristic rise time decreased as expected with increasing intensity: $\tau_{\text{As}_2\text{Se}_3}^r = 95I^{-0.95} \text{ s}$ and $\tau_{\text{As}_2\text{S}_3}^r = 630I^{-0.9} \text{ s}$ where I is the average intensity in the layer calculated with the transfer matrix method (TMM).^{10,11} The characteristic decay time after 2 min illumination in-

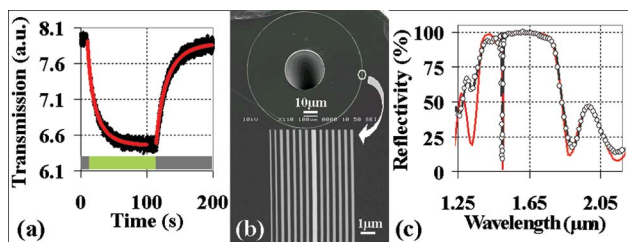


Fig. 1. (a) *In situ* transmission measurements at $1.5\ \mu\text{m}$ on a 100-nm-thick As_2Se_3 film (black curve) and fitting with a stretched exponential function (red curve). Illumination and dark times are indicated in green and gray, respectively. The intensity in the layer was $\sim 16\ \text{mW}/\text{cm}^2$. (b) Scanning electron micrographs of the cross section of a $910\text{-}\mu\text{m}$ -diameter fiber showing the As_2Se_3 cavity layer (bright gray in the middle of the structure), the As_2S_3 layers (intermediate gray) and the polymer layers (dark gray). (c) Measured (black line with dots) and computed (red line) reflectivity spectra for the $910\text{-}\mu\text{m}$ -diameter fiber. Fourier transform spectroscopy and NBR measurements have been superimposed.

creased with increasing intensity as $\tau_{\text{As}_2\text{Se}_3}^d = 9.5 \exp(0.04I)\ \text{s}$ and $\tau_{\text{As}_2\text{S}_3}^d = 6.6 \exp(0.02I)\ \text{s}$, indicating that holes diffuse further from the illumination region.

The fiber structure was designed to achieve a high- Q Fabry–Perot cavity while optimizing the material distribution to maximize the shift of the cavity’s resonant mode under illumination.¹² The optimal solution consisted of placing As_2Se_3 in the cavity layer, because the material’s high absorption coefficient at $514\ \text{nm}$ [$k=0.6047$ (Refs. 13 and 14)] resulted in a larger and faster response, and using As_2S_3 for the numerous mirror layers because its smaller absorption coefficient [$k=0.0072$ (Refs. 13 and 14)] permitted a higher pump light intensity in the cavity layer. The cross section of a $910\text{-}\mu\text{m}$ -diameter fiber prepared with a JEOL (CP)SM-09010 cross-section polisher was observed by scanning electron microscopy. The fiber was composed of a hollow-core PEI rod surrounded by 6+7 bilayers of As_2S_3 and PEI, separated by an As_2Se_3 layer that formed the Fabry–Perot cavity [Fig. 1(b)]. Two extra polymer layers protected the fiber surface. The preform fabrication technique and the fiber drawing conditions have been described elsewhere.^{2,15} The As_2S_3 layers were $\sim 190\ \text{nm}$ thick, the PEI layers were $\sim 210\ \text{nm}$ thick, and the defect layer was $\sim 250\ \text{nm}$ thick.

Reflectivity measurements were performed using a Tensor 37 Fourier transform infrared spectrometer coupled to a Bruker Hyperion 2000 IR microscope with a lens numerical aperture corresponding to 30° of angular spread [Fig. 1(c)]. Because of the optical cavity small field of view,¹⁶ we also performed narrowband reflectivity (NBR) measurements using a Photonics Tunics plus tunable laser emitting from 1.49 to $1.62\ \mu\text{m}$. The beam was sent on the fiber at normal incidence, and a beam splitter was used to direct half of the reflected beam to a Newport 818IG InGaAs detector placed $1.5\ \text{m}$ from the fiber, corresponding to an effective collection angular range $<0.01^\circ$ and a minimal signal-to-noise ratio of 20 [Fig.

2(a)]. By use of the n and k values of As_2S_3 , As_2Se_3 , and PEI measured by spectroscopic ellipsometry,¹³ the reflectivity spectra of these fibers were computed with the TMM and averaged over the experimental incidence angle and polarization range. While we obtained good agreement with the FTIR measurements [Fig. 1(c)], the NBR measurements exhibited a cavity resonant mode that was broader and less deep than the calculated one, leading to a quality factor equal to 225, $\sim 35\%$ lower than the theoretical one [Fig. 2(b)]. This indicates the presence of unaccounted materials and radiation loss most likely as a result of interface roughness and layer thickness fluctuations that affect the reflectivity of the mirror layers at the resonant wavelength.¹⁷

We measured the photoresponse of these fibers by performing *in situ* NBR measurements [Fig. 2(a)]. The incident angle of the Ar^+ laser was tuned around 20° , corresponding to the theoretical maximum penetration of the multilayer structure. The fiber was initially illuminated for 2 h to ensure saturation of MP. The reflected power before and under illumination was then measured at each probe wavelength with illumination and dark times equal to 1 and 2 min, respectively. We measured a photoinduced shift of the cavity resonant mode of the $910\text{-}\mu\text{m}$ -diameter fiber by $2\ \text{nm}$ under $574\ \text{mW}/\text{cm}^2$ illumination, corresponding to a maximum change in reflectivity of 58% at $1497.5\ \text{nm}$ [Fig. 2(b)]. Using the intensity dependence of the amplitude and kinetics of TP and the TMM to calculate the profile of the pump light intensity in the chalcogenide glass layers,¹⁰ we computed a theoretical shift of the cavity resonant mode equal to $2.2 \pm 0.3\ \text{nm}$ under similar illumination conditions. Possible sources of error included the uncertainty of

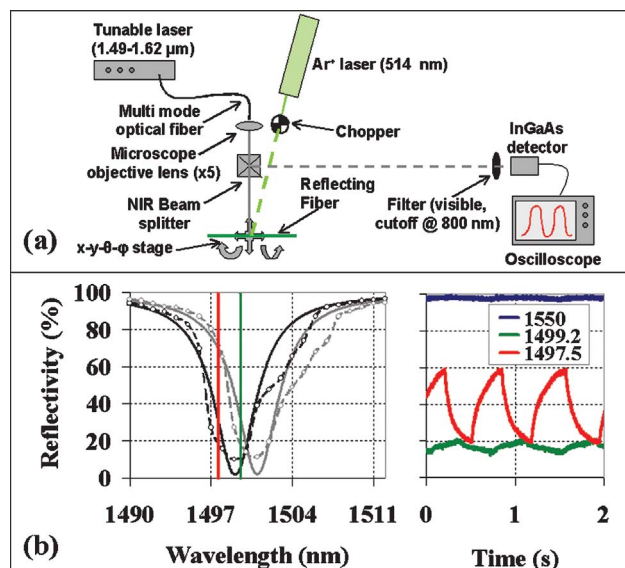


Fig. 2. (a) NBR and optical tuning experimental setups. (b) Left, shift of the cavity resonant mode to higher wavelengths under $574\ \text{mW}/\text{cm}^2$ illumination. The dashed curves with dots correspond to NBR measurements; the solid curves correspond to TMM simulations. Right, $1.5\ \text{Hz}$ modulation of the reflected power at three different probe wavelengths. 1497.5 and 1499.2 are indicated on the NBR spectra by red and green lines, respectively.

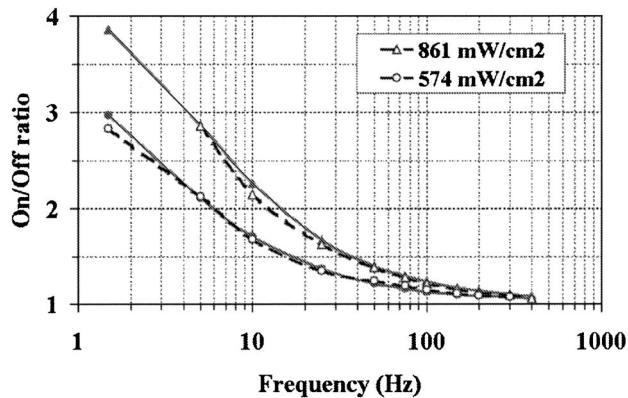


Fig. 3. Measured (dashed black curves) and computed (gray solid curves) on–off ratios at 1497.5 nm for frequencies up to 400 Hz under two illumination powers.

the actual incident power because of the cylindrical geometry of the fiber and rough interfaces, the uncertainty of the amplitude of the TP in the chalcogenide fiber layers compared with that in the thin films, and uncertainty of the refractive index of the materials, especially the k values of As_2Se_3 at 514 nm. Because of the poor thermal conductivity of the polymer layers, the glass layers were subjected to moderate heating under illumination, $<35^\circ\text{C}$ at the fiber surface (measured with a forward-looking infrared camera) and $<5^\circ\text{C}$ in the cavity layer (estimated). The corresponding thermal expansion was well below 0.01% for all layers.

To characterize the dynamic behavior of the optical tuning, we connected the detector to a Tektronic TDS 3032B oscilloscope and modulated the pump light intensity with a chopper [Fig. 2(a)]. The wavelength dependence of the modulation amplitude [Fig. 2(b)] was a clear indication that it was induced by a shift in the spectral position of the cavity resonant mode. At 1.5 Hz, the maximum change in reflectivity was equal to 41% at the cavity edge under 574 mW/cm^2 illumination. In Fig. 3 we report the on–off ratios at 1497.5 nm (ratio of the reflected power with and without pump light illumination) under 574 and 861 mW/cm^2 illumination for frequencies up to 400 Hz. Increasing the pump light intensity to 861 mW/cm^2 significantly increased the on–off ratios because of a faster and larger index change in the fiber cavity and mirror layers, while a further increase did not result in any improvement because of an increase in the decay times of the TP and material losses. We used the TMM and the characteristics of the TP to compute the expected on–off ratios under similar experimental conditions and obtained very good agreement with the measurements (Fig. 3). Dynamic tuning was limited by the Fabry–Perot cavity Q factor and the fundamental response time of the materials, while the on–off ratios were penalized by the high reflectiv-

ity at the resonant wavelength. These results can be improved by increasing the number of bilayers and selecting more efficient materials.

The authors thank S. D. Hart, D. Sadoway, R. Sun, JEOL Ltd. Japan, Y. Kuriki, and D. Hinczewski for their help. This work was supported by the Defense Advanced Research Projects Agency/Griggs (contract HR-0011-04-1-0003), the Army Research Office through the Institute for Soldier Nanotechnologies (contract DAAD-19-02-D-0002), the U.S. Office of Naval Research (contract N00014-02-1-0717), the Air Force Office of Scientific Research (contract Y77011), and the National Science Foundation (contract ECS-0123460). This work was also supported in part by the Materials Research Science & Engineering Centers Program of the National Science Foundation under award DMR 02-13282. Y. Fink's e-mail address is yoel@mit.edu.

References

1. P. R. Villeneuve, S. Fan, and J. D. Joannopoulos, *Phys. Rev. B* **54**, 7837 (1996).
2. G. Benoit, S. D. Hart, B. Temelkuran, J. D. Joannopoulos, and Y. Fink, *Adv. Mater.* **15**, 2053 (2003).
3. S. Fan, W. Suh, and M. F. Yanik, *Proc. SPIE* **5280**, 134 (2004).
4. T. D. Engeness, M. Ibanescu, S. G. Johnson, O. Weisberg, M. Skorobogatiy, S. Jacobs, and Y. Fink, *Opt. Express* **11**, 1175 (2003).
5. G. Pfeiffer, M. A. Paesler, and S. C. Agarwal, *J. Non-Cryst. Solids* **130**, 111 (1991).
6. A. Ganjoo and K. Shimakawa, *J. Optoelectron. Adv. Mater.* **4**, 595 (2002).
7. H. G. Tompkins and W. A. McGahan, *Spectroscopic Ellipsometry and Reflectometry: a User's Guide* (Wiley, 1999).
8. A. C. van Popta, R. G. DeCorby, C. J. Haugen, T. Robinson, and J. N. McMullin, *Opt. Express* **10**, 639 (2002).
9. K. Petkov, *J. Optoelectron. Adv. Mater.* **4**, 611–629 (2002).
10. P. Yeh, A. Yariv, and C.-S. Hong, *J. Opt. Soc. Am.* **67**, 423 (1977).
11. M. Born and E. Wolf, *Principles of Optics* (Pergamon, 1970).
12. J. D. Joannopoulos, R. D. Meade, and J. N. Winn, *Photonic Crystals: Molding the Flow of Light* (Princeton U. Press, 1995).
13. G. Benoit, Electronic database: <http://mit-pbg.mit.edu/Pages/DataBase.html> (MIT, 2005).
14. Electronic Handbook of Optical Constants of Solids (SciVision, 1999).
15. S. D. Hart, G. R. Maskaly, B. Temelkuran, P. H. Prideaux, J. D. Joannopoulos, and Y. Fink, *Science* **296**, 510 (2002).
16. P. Yeh, *Optical Waves in Layered Media* (Wiley, 1988).
17. B. E. A. Saleh and M. C. Teich, *Fundamentals of Photonics* (Wiley, 1991).